PROGRESSIVE FAILURE AND REHABILITATION OF RC DECK SYSTEMS WITH COMPOSITES

Kumar K. Ghosh*, Vistasp M. Karbhari**
*California Department of Transportation, **University of California San Diego

Keywords: *rehabilitation; external bonding; slabs; punching shear; NDE*

Abstract

This paper presents the results of a two-pronged investigation aimed at studying the rehabilitation of bridge decks at the "systems level" through use of a three-girder bridge deck system. The objective of the study is to evaluate the damage progression in the deck slabs and the longitudinal girders under wheel load applications and to detect changes in the overall response of structure caused by the strengthening of only individual components that pushes the other components towards critical levels. The deck slab-girder system is tested to simulate behavior under field loading in which the deck slabs are found to be susceptible to punching shear type failures and the longitudinal girders are usually found to be deficient in terms of shear demand. NDE techniques, involving infra-red thermography and modal testing are evaluated as means to identify the shifts in damage localization, overall response and damage progression caused by subsequent modifications to the structure.

1 Introduction

Fiber reinforced polymer (FRP) composites are increasingly being accepted for use in external strengthening of deteriorating and under-strength concrete structures. However, to date most studies have been at the level of single components without a detailed study of systems level effects and the effect of progressive damage. In addition there has been very little study of non-destructive techniques to evaluate the performance of the rehabilitated structure over its useful life and to monitor any progression of damage or change in load paths between the structural components.

In a number of cases longitudinal girders of the structural systems have reinforcement details such that they will have sufficient reserve capacity at the load level where the deck slabs would reach their critical limit state, usually in terms of punching shear capacity. Hence most of the damage, in these cases, at the initial load levels is concentrated in the deck slabs with the longitudinal girders having little or no damage. Thus the general trend has been to strengthen only the deck slabs with FRP composite strips bonded to the bottom surface of the slabs. However after the slabs are strengthened, the bridge deck will be able to withstand higher loads and this increases the load demands on the longitudinal girders. An effective punching-shear strengthening scheme in the slabs will reduce the opening of cracks and very little damage will occur in the slabs at these load levels until the composite strips reach debonding strain levels. Thus most of the damage will be localized in the un-strengthened longitudinal girders and depending on the section and reinforcement details will push them towards flexural or shear criticality before the full capacity of the strengthened deck slabs can be reached. This creates a secondary deficiency which could result in premature failure of the rehabilitated system. In order to enable full utilization of the enhanced strength of the deck slabs the capacity of the girders needs to be also assessed and may require strengthening.

This aspect of systems level response change due to local rehabilitation has not been studied to an appreciable extent and is a major weakness in the study of external bonded FRP rehabilitation of deteriorating and deficient concrete structural systems. In addition there has been very little study of non-destructive techniques to evaluate the performance of the rehabilitated structure over its useful life and to monitor any progression of damage or change in load paths between the structural components, making a true assessment of the viability and efficacy of FRP rehabilitation at the systems level incomplete. It is emphasized that rehabilitation must not just result in the local strengthening or repair of a component, but must

necessarily also not result in redistribution of load to cause unintended premature failure in other non-rehabilitated components, nor should it cause a deteriorative change at the systems level.

This paper provides results of an investigation that assesses progression of failure between components due to rehabilitation.

2 Experimental Program

2.1 Test Specimen

The test specimen consists of a three-girder two bay bridge deck segment with center-to-center distance between the longitudinal girders of 1.68 m (5.5 feet) and a slab thickness of 152 mm (6"). The girders had a total depth (including the slab flange) of 559 mm (22") and width of 203 mm (8"). The total longitudinal span length of the specimen is 3.6m (12'4"). An overhang of 607 mm (24") was also constructed on either side of the longitudinal edge girders. Details of specimen geometry are shown in Figure 1.
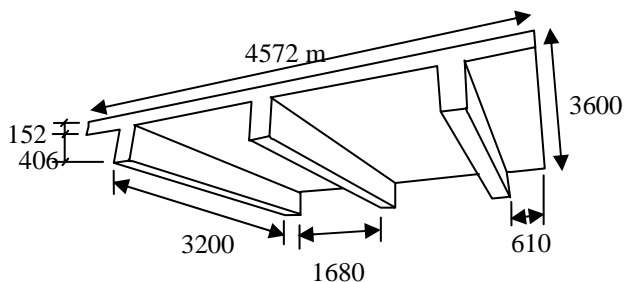

Fig. 1: Overall configuration (all dimensions in mm)

The main transverse reinforcement in the slabs consisted of #5 bars spaced at 203 mm center-to-center and the main longitudinal reinforcement consisted of #5 bars spaced at 406 mm, which resulted in a longitudinal to transverse reinforcement ratio of 2. This design simulated pre-1970 designs of slab-girder bridges in which typically a transverse to longitudinal reinforcement ratio of 2 was also used. This was observed in the slab sections cut-off from the Watson Wash Bridge and tested earlier [1,2] in which, the transverse reinforcement consisted of #5 rebars spaced at 140 mm and the longitudinal reinforcement consisted of #5 rebars spaced at 280 mm. However the spacing of the main transverse reinforcement in the test specimen was chosen to be about 1.5 times larger than the spacing of pre-1970 representative bridge deck [203 mm as compared to 140 mm] to cause a reduction of the maximum

positive moment capacity of the slabs in the test specimen with respect to a typical pre-1970 bridge deck slab at construction by about 30%. This was done to take into account the lower concrete strengths used in pre-1970 design and construction of bridges as well as to take into account the degradation of such existing deck slabs over time caused by environmental exposure and continued traffic loading. It should be noted that a transverse to longitudinal reinforcement ratio of 2 along with ratio of longitudinal span length to distance between the longitudinal girders greater than 2 in typical existing slab-girder bridge decks would result in one-way load transfer mechanism, in which the load from the slabs would be transferred directly to the longitudinal girders and thereby to the abutments.

For the girders, #9 and #11 bars were used for the longitudinal reinforcement and #3 bars were used for the stirrups. The reinforcement details are presented in Figure 2. The specific stirrup spacing, and high longitudinal reinforcement ratio were used in the girders to simulate shear deficiency in the middle girder. A closer stirrup spacing of 76 mm was used near the support regions of the middle longitudinal girder to avoid an undesirable premature local failure in this region. This was because the test specimen was supported on load cells placed at each end of the girders and the shear demand was highest at these locations. However in the case of shear strengthening of the middle longitudinal girder with externally bonded U-shaped FRP composite stirrups, the presence of the load cell below the girder at the support makes it impossible to use a continuous U-stirrup to wrap around the web of the beam at the support locations. Thus the closer internal steel stirrup spacing of 76 mm was used at the support so that the shear capacity at the support even without the composite strengthening was higher than the maximum design shear demand. The longitudinal reinforcement was kept similar in all the three girders to ensure that none of the girders would fail in flexure. However on account of lower shear demand on the edge girders a uniform stirrup spacing of 305 mm was used. Grade 60 steel was used for all the reinforcing bars.

The entire specimen was cast in formwork on the ground and then lifted into place. A detailed characterization program was conducted for materials to provide data both in the as-built condition, and in the case of concrete, as a function of the age of the concrete, and detailed results are presented in [3].
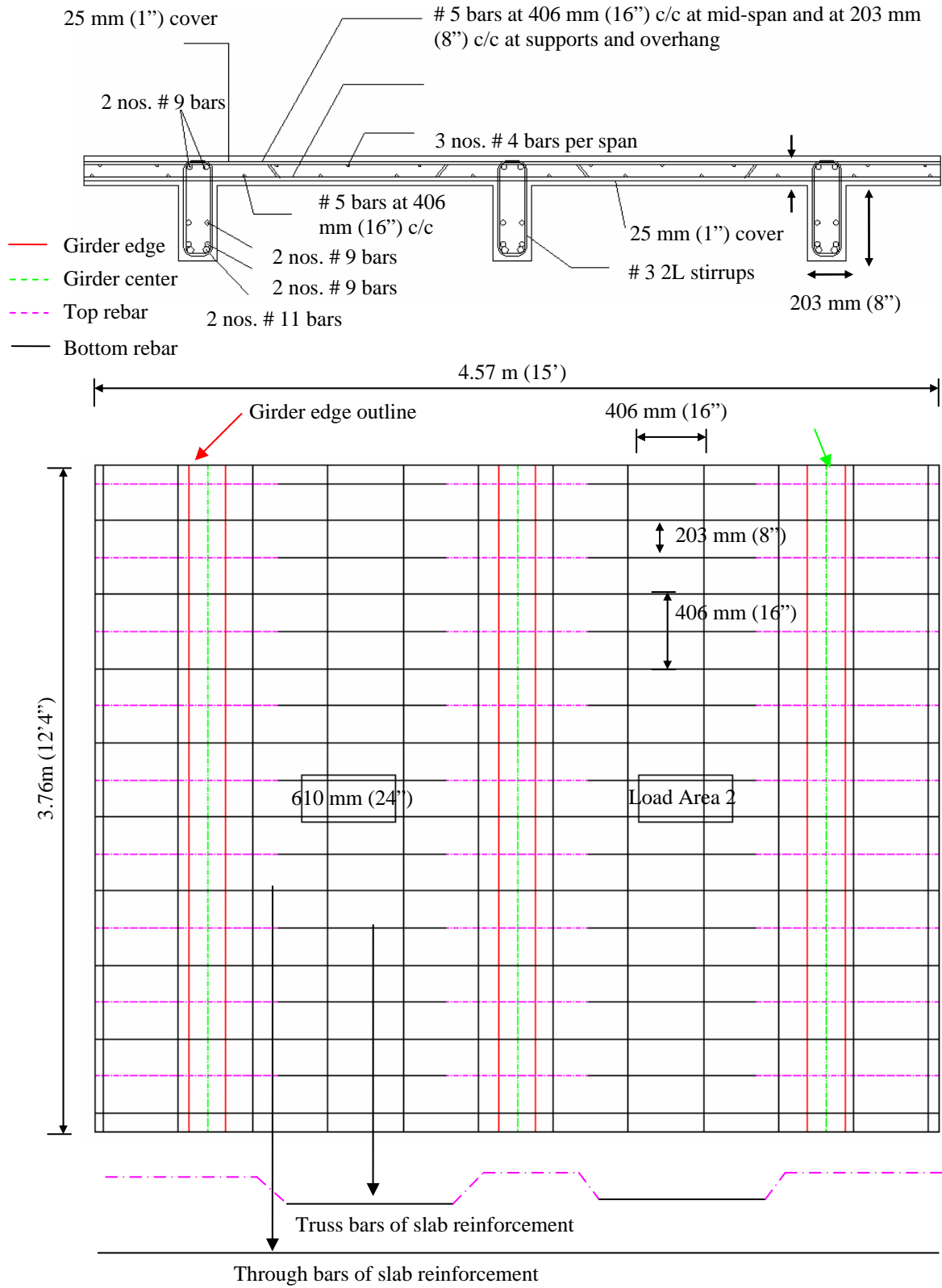
25 mm (1") cover

\# 5 bars at 406 mm (16") c/c at mid-span and at 203 mm (8") c/c at supports and overhang

2 nos. \# 9 bars

3 nos. \# 4 bars per span

Girder edge

Girder center

Top rebar

Bottom rebar

\# 5 bars at 406 mm (16") c/c

2 nos. \# 9 bars

2 nos. \# 9 bars

2 nos. \# 11 bars

25 mm (1") cover

\# 3 2L stirrups

203 mm (8")

4.57 m (15')

Girder edge outline

406 mm (16")

203 mm (8")

406 mm (16")

3.76m (12' 4")

610 mm (24")

Load Area 2

Truss bars of slab reinforcement

Through bars of slab reinforcement

Fig. 2: Reinforcement Details

2.2 Setup and Loading Protocol

The center-to-center distance between the supports in the longitudinal direction was 3.2 m (10.5 feet). The specimen was tested under monotonically increasing load applied by two 979 kN (220 kips) capacity hydraulic actuators and the load was cycled at predetermined levels to check for structural stability and to perform NDE. The load from the actuators was transferred to the test specimens through load bearing plates having a loading footprint area of 508 mm (20 inches) x 254 mm (10 inches) that represents typical design wheel load contact areas. The center-to-center distance between the load contact areas was used as 1.83 m (6 feet) to simulate typical design axle distance of a permit truck. A 76.2 mm (3-inch) thick elastomeric bearing pad was also placed between the load bearing plates and the concrete surface to obtain a uniformly distributed constant pressure on the slab. The test setup is presented in Figure 3.

Fig. 3: Test Setup

The test program is carried out in three phases, in which phase 1 involves loading to initiate cracking in the slabs and cause them to reach predetermined level of damage. This level was chosen as 75% of transverse steel yield or 75% of the shear capacity of the slabs whichever is smaller. Such a load level for was deemed to be representative of deterioration in the deck slab that will warrant rehabilitation/strengthening of the slab with FRP composites to prevent further degradation and failure. However, at this level of loading, the girders will not reach critical capacities and thus will not need any strengthening. At the end of phase 1 of

testing the slabs are strengthened with externally bonded FRP composite strips. Phase 2 involves loading to initiate damage in the middle longitudinal girder, as it tends to reach its critical limit state in shear. Strains in the range of 75% of yield in the internal steel stirrups will be deemed to warrant shear strengthening of the girder with FRP composite U-wraps with composite anchors. The shear strengthening of the girder allows the deck system to resist higher load levels and Phase 3 involves further loading of the test specimen until the strengthened slabs reach their flexural capacity governed by debonding of the composite strips and ultimate failure of the test specimen due to punching shear failure of the deck slabs. The progression and localization of damage in the deck slabs and the girder are assessed using NDE techniques at beginning and end of each phase as well as at intermediate load levels.

2.3 Nondestructive Evaluation

Forced excitation based dynamic modal testing was carried out both at the beginning and end of each phase as well as at intermediate load levels through each of the phases. The objective of the vibration tests is three-fold: i) To use system identification technique to calibrate initial finite element model based on dynamic characteristics like natural frequencies (and mode shapes); ii) To use system ID and model updating to calibrate subsequent finite element models corresponding to various damage states and identify the impact of damage or strengthening on the structure; iii) To detect appearance and progression of damage as well as determine damage severity using damage detection algorithms based on frequencies and/or mode shapes. System ID is the primary focus of the vibration tests for this project but attempts are made to use damage detection techniques to locate damage areas and determine their severity. This will help to evaluate the effectiveness of modal testing to be used as a health monitoring/NDE technique for RC slab and girder bridges at the system level.

The objective of using IR Thermography in the current test program is two-fold, one being the detection of any pre-existing defect/damage areas in the composite strips and the other being the characterization of damage progression in the strips with loading. Inspection was carried out before the start of phase 2 of testing for both the strengthened

slabs to form the baseline for subsequent inspections. The data is acquired using a thermographic NDT system. Flash heating provided by 2 xenon flashtubes with 5 ms flash duration, each powered by a 6.4 kJ capacitor bank is used to simulate temperature differential between the composite and any potential debond / delamination areas. An infrared camera operating in the 2 – 5 μm spectral range is used and continuous 12 bit data is acquired at a 60 Hz frame rate for 10 sec after flash heating for each shot.

2.4 FRP Rehabilitation

The slabs were rehabilitated with FRP composites after reaching the pre-defined damage state. One slab each, was rehabilitated using adhesively bonded prefabricated strips and site-impregnated unidirectional carbon fabric laminates. Typical properties are given in Table 1

TABLE 1: FRP Material Characteristics

Composite Type		Unidirectional Fabric			Strip
		1 layer	2 layers	3 layers	
Thickness mm	Mean	1.67	3.13	4.20	1.37
	Std. Dev.	0.15	0.29	0.18	0.01
Strength MPa	Mean	717.40	692.50	588.86	2142.62
	Std. Dev.	88.70	112.01	43.87	221.50
Modulus GPa	Mean	46.0	50.77	53.14	137.64
	Std. Dev.	7.77	7.88	6.44	11.87

3 Results

3.1 Phase 1 Loading

The theoretical punching shear capacity computed using AASHTO design equation [4] was 534 kN. The initial and longitudinal and transverse cracks below the load areas were observed at 214 kN. With further loading the cracks diverged diagonally away from the load area towards the ends of the girders indicating punching shear deficiency in the slabs (Figure 4). Also the strains in the transverse steel reinforcement of the slabs were less than 40% of yield strain (Figure 5). The first hairline shear cracks in the middle longitudinal girder were observed around 356 kN. At 400 kN the slabs had extensive cracking and since this load also corresponded to 75% of punching shear capacity,

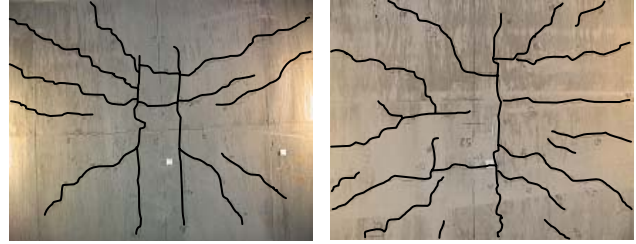loading was stopped and the slabs were strengthened with FRP composite.

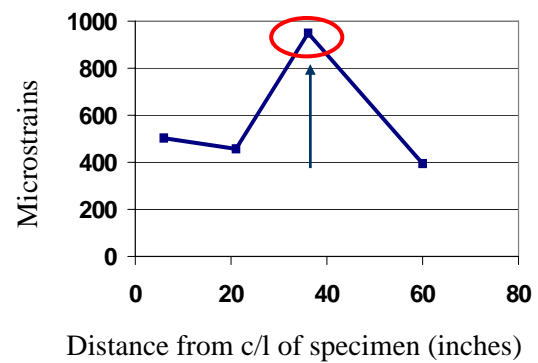Fig. 4: Crack Patterns in the two slabs

Fig. 5: Strain in transverse steel rebar below load area of slab 1

3.2 Phase 2 Loading

Two strengthening schemes were used for the two deck slabs, namely FRP composites in the form of site impregnated carbon fabric laminates and prefabricated carbon epoxy strips, to test the comparative effectiveness of the two systems. The design was based on the criteria of having a strength enhancement ratio of 2 and to have the strain in the composite within reasonable bounds to restrain the opening of the cracks in the deck slabs. Based on the properties obtained from material tests and limiting debonding strains of 3674 and 3278 microstrains computed from a debonding strain prediction model [5], the strengthening in slab 1 was computed as 1 layer of prefabricated strip at 381 mm center-to-center in both the longitudinal and transverse direction. Slab 2 was designed to be strengthened with site impregnated fabric laminates with 2-layers spaced at 533 mm in the transverse direction and with 1-layer spaced at 381 mm in the longitudinal direction. Different spacing for the two systems was used to obtain equivalent transverse flexural capacity. The installation procedure simulated field practices and the strengthening schemes are

presented in Figure 6. Phase 2 testing was started after the composite was allowed to cure for a week.

Fig. 6(a): Section of deck rehabilitated with prefabricated strips

Fig. 6(b): Section of deck rehabilitated with wet layup of unidirectional fabric

In Phase 2 the specimen was loaded to 667 kN at which point the middle girder was predicted to reach shear criticality. Shear cracks were observed in girder near support areas (Figure 7) and the strain in the steel stirrups reached ~ 75% of yield strain (Figure 8).

Fig. 7: Shear cracks in the girder

Loading was stopped and the girder was strengthened with 3 layers of CFRP composite U-stirrups at a spacing at which the strengthened girder was predicted to have a shear capacity exceeding the demand at failure of the strengthened slabs. Glass fiber bundles impregnated with resin were installed through holes drilled in the chamfer of the girder and were splayed between the second and third CFRP layers to anchor the composite stirrups (Figure 9).
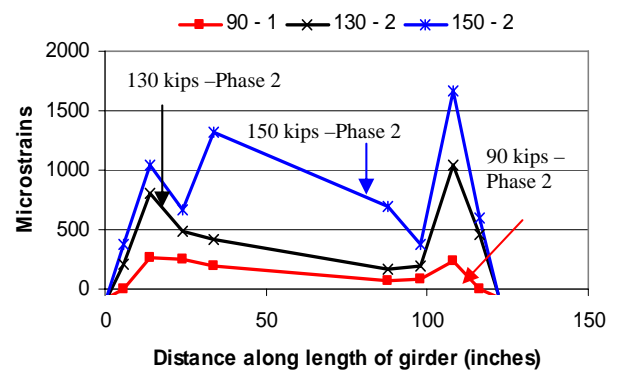
Fig 8: Strain in girder stirrups

Fig 9: Placement of FRP stirrups and anchors

At this stage the strains in slab composite were below predicted debonding strains. Also after strengthening, there was a reduction in the mid-span deflection by 15% and reduction in the strain in the

transverse steel below the load area by ~25% from the test data obtained at 400 kN, indicating effectiveness of the composite strengthening schemes.

3.3 Phase 3 Loading

In Phase 3 the specimen was loaded to failure of the strengthened slabs predicted to occur at 934 kN. In both the slabs the failure was initiated by debonding of the composite strips at the locations of the primary punching shear cracks. Load-deflection response as measured under the central girder with a comparison to the end of Phase 2 loading is shown in Figure 10.
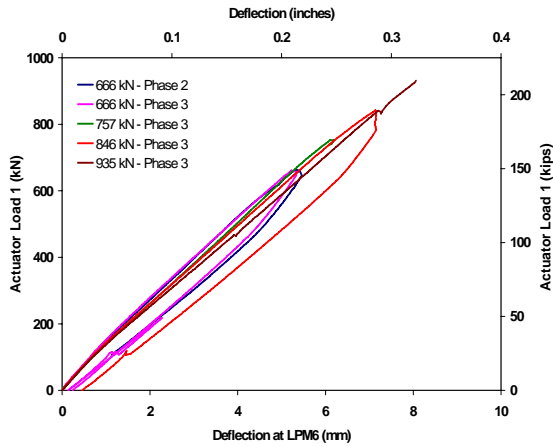
Fig. 10: Load-deflection response under the middle girder

The strain profiles in the composite are presented in Figures 11(a) and 11(b) and the measured debonding strains were 3526 μs and 3354 μs, for the prefabricated strips and the fabric laminates respectively, which compared well with the predicted debonding strains. The debonding of the composite was followed by punching shear failure around 934 kN, as predicted. In slab 1 at failure there was large opening of cracks around the punching shear perimeter and some of the prefabricated strips had interlaminar failure. For Slab 2, failure was more gradual and the larger punching shear perimeter indicated load distribution over a wider area. Also at end of phase 3 loading, the composite stirrups in the girder had strains below debonding strains indicating effectiveness of the composite in shear strength enhancement.
No new cracks appeared in the deck slabs over the load cycles of phase 3. Both the composite systems were effective in restraining the opening of the existing cracks and thus prevented the occurrence of

punching shear failure. Typical visual inspections of the deck slabs are presented in Figure 12.
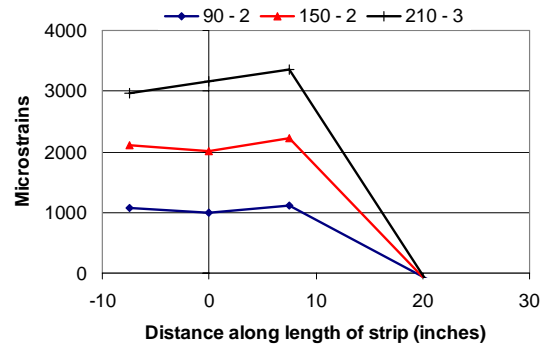

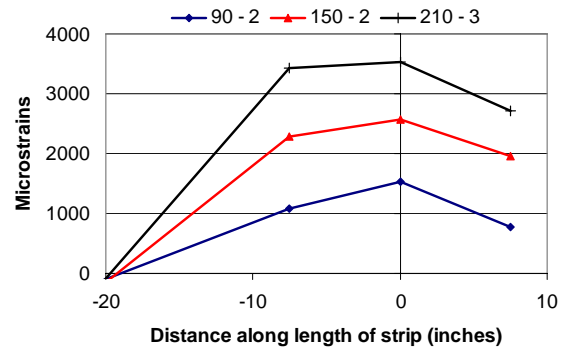Fig. 11(a): Strain along transverse composite below load in Slab 1

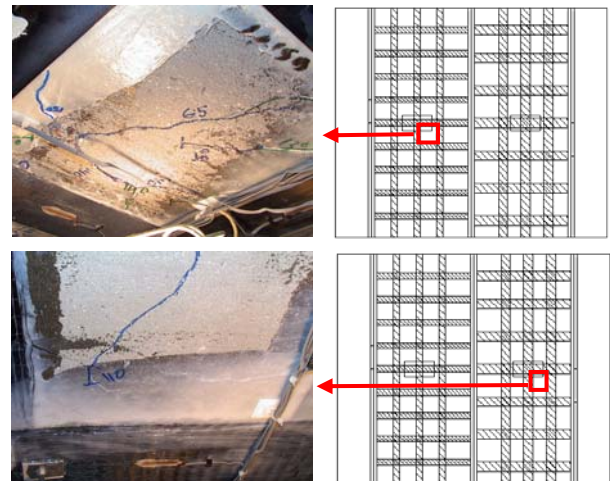Fig. 11(b): Strain along transverse composite below load in Slab 2

Fig. 12: Damage in slabs at edges

The cracks were visible only in the unstrengthened area of the slabs and no visual damage was evident in the composite at the areas where they intersected the cracks. Continuous popping sounds were heard throughout the load

cycles of phase 3 as the epoxy at the borders of the composite strips/laminates cracked at the locations of the cracks. Also at 846 kN cracks were observed on the top surface of the specimen in the negative moment area of the slabs along the center girder. Cracks were also found to develop at this load level at the intersections of the slabs and the edge girders. The measured crack widths on the top surface of the specimen over the center girder and at the slab-girder intersection regions were approximately 1 mm and 0.6 mm, respectively, and thus the damage was not considerable. However the cracks were indicative of the initiation of damage in the slab-girder system with further loading. This was because since the slab and girder components of the slab-girder system were strengthened, the damage was localized in the next weak link of the slab-girder system at the slab and girder joints.

The debonding of the composite strips/laminates in the two slabs occurred simultaneously at 933 kN. Since the debonding of the composite resulted in loss of the strength enhancement of the slabs produced by the composite, the slabs could not resist the high wheel load demands. Since the ultimate punching shear capacity of the unstrengthened deck slabs was predicted to be 534 kN, as soon as debonding of the composite occurred at a load of 935 kN, which was 1.75 times higher than the unstrengthened punching shear capacity, the debonding was followed by simultaneous punch through of the load pad, representing the wheel load, through the concrete. All the composite areas at the intersection with the punching shear cracks were debonded at failure load. This included the areas in the longitudinal strips/laminates intersected by the cracks propagating in the transverse directions. The cracks propagating in the longitudinal direction intersected the transverse strips/laminates at the edges and caused debonding of the composite at these locations. Representative regions of failure in the two strengthened slabs are presented in Figures 13 and 14. However the mode of debonding was different in the two composite systems. The larger width of the fabric laminates resulted in gradual and smaller opening of the punching shear cracks. There were very few severely debonded areas and most of the debonding was localized at intersections with the punching shear cracks.

In contrast, for the prefabricated strips, large areas of the strip in the vicinity of the punching shear cracks were debonded.
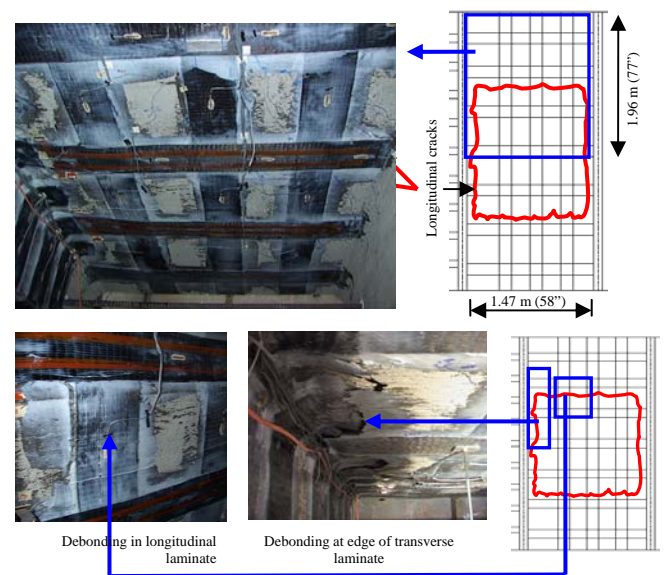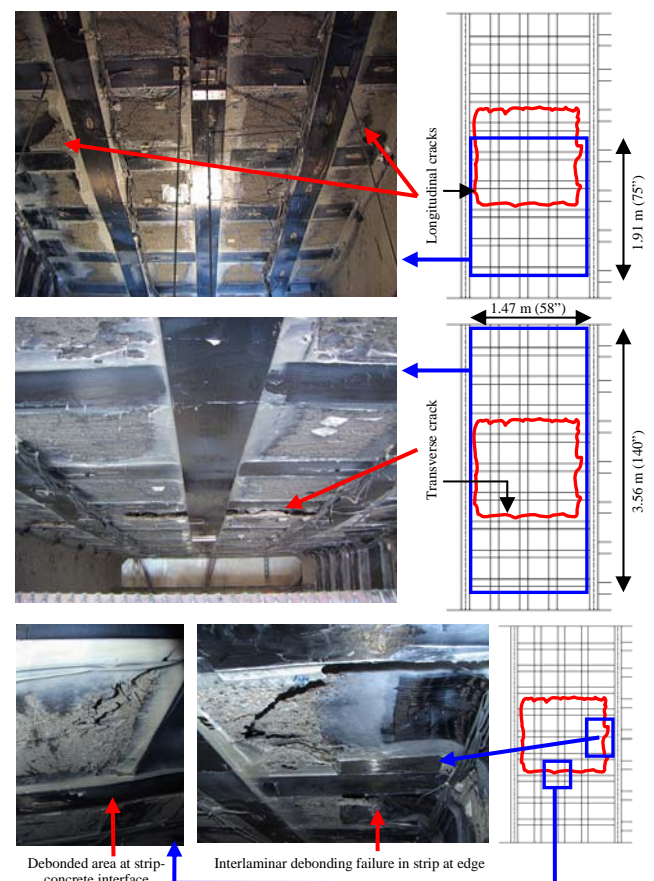

Fig. 13: Damage in slab 2

Fig. 14: Damage in slab 1

Also at many locations of the debonded composite, the failure was interlaminar inside the composite strip itself rather than at the composite-concrete interface. This indicated that the

interlaminar bond strength of the prefabricated strip was lower than the bond strength between the composite and the concrete. This resulted in a more abrupt mode of debonding with large opening of the punching shear cracks as compared to the fabric laminates.

Both the slabs reached their ultimate capacity at 933 kN which matched the predicted ultimate capacity of 935 kN [3]. The simultaneous failure of the two slabs also indicated that equivalent capacity was achieved using the two different composite systems. The degradation of slab stiffness was gradual over the loading stages which was representative of a flexural behavior. Thus the strengthening of the deck slabs with composite was effective in restraining the opening of existing cracks and in preventing the occurrence of punching shear failure. The slabs reached their ultimate capacity at predicted debonding strains in the composite strips/laminates. The highest strains recorded in the transverse strips and laminates below the load area at 933 kN were 3430 and 3353 micro-strains, respectively which matched well with the predicted ultimate debonding strains of 3568 and 3262 micro-strains for the prefabricated strips and fabric laminates respectively. Once the slabs had reached their flexural capacity, punching shear cracks opened up resulting in ultimate failure. The shear strengthening of the center girder with composite stirrups resulted in shear strength enhancement and control of opening of shear cracks in the girder. None of the composite stirrups reached debonding strains at failure of the deck slabs.

In this phase of test, after the slabs and the girder were strengthened with composite at the component level, the damage was localized at the slab–girder intersection region. This resulted in the formation of cracks running on top of the slab at the negative moment area near the slab-girder intersection area. Through thickness cracks running through the slab were also visible in this region at the outer edge of the specimen. This indicated that at the system level after strengthening of the slab and girder for higher load demand, it would be necessary to take into account the design of the joint to prevent localized failures that might prevent the strengthened components to reach their ultimate capacities.

3.4 Forced Excitation Based Modal Testing

The inspections were carried out both at the beginning and end of each phase as well as at intermediate load levels. The objectives of the vibration tests were: i) To use system ID technique to calibrate initial finite element model based on dynamic characteristics like natural frequencies (and mode shapes); ii) To use system ID and model updating to calibrate subsequent finite element models corresponding to various damage states and identify the impact of damage or strengthening on the structure; iii) To detect appearance and progression of damage as well as determine damage severity using damage detection algorithms based on frequencies and/or mode shapes. The FRF magnitude plots obtained over the three phases of loading are shown in Figures 15 (a)-(c). The frequency ratio, defined as the ratio of the frequency obtained at a particular load stage to the baseline frequency of the structure obtained prior to loading, was used to provide an estimate of the change in the natural frequency of the structure as compared to the baseline frequency of the virgin structure, caused by damage/strengthening over the load stages, and is presented in Figure 16.
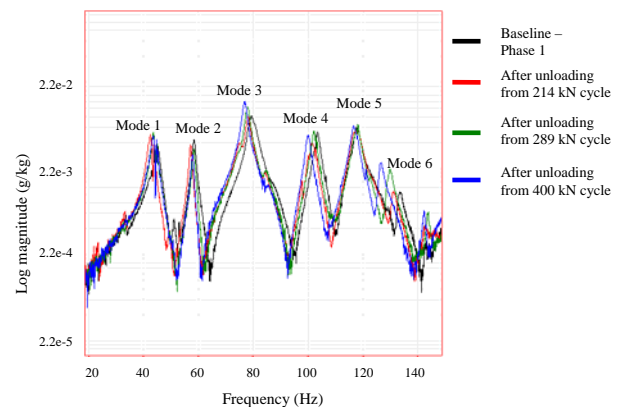

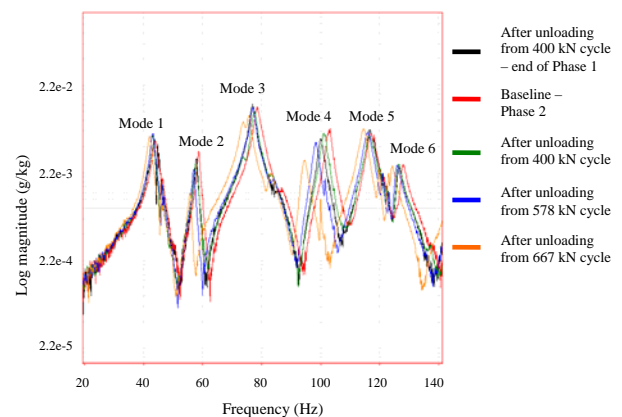Fig. 15(a): FRF magnitude plots for Phase 1 of testing

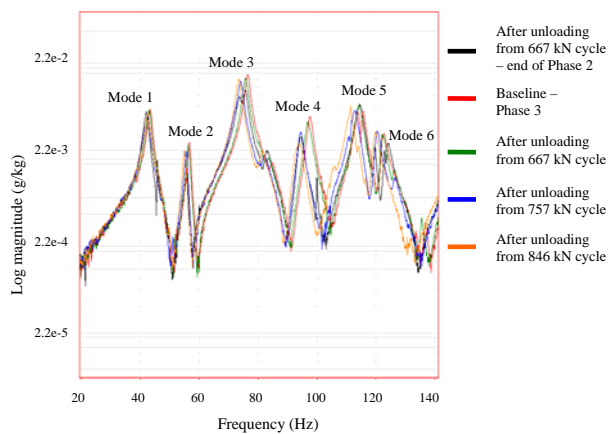Fig. 15(b): FRF magnitude plots for Phase 2 of testing

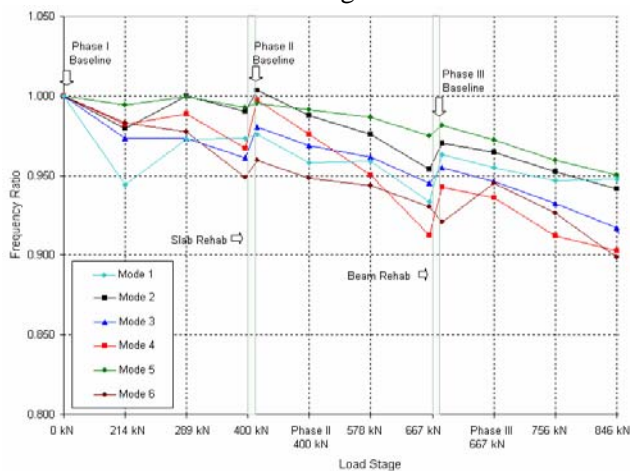Fig. 15(c): FRF magnitude plots for Phase 3 of testing

Fig. 16: Trend of frequency ratio over the load stage

A general trend of decrease of the natural frequency was observed over all the load stages indicative of damage progression in the test specimen since the frequency is directly related to the stiffness of the structure. Also an increase of the natural frequency was observed corresponding to results from baseline 2 and baseline 3, obtained after strengthening of the deck slabs and the center girder, respectively. However the stiffness degradations/enhancements in specific components of the structure due to damage/strengthening leading to such frequency changes could only be identified through model updating.

3.5 IR Thermography

The objectives of IR Thermography were to detect pre-existing defect areas in the composite produced during installation and to characterize damage progression in the composite with loading. Inspection was carried out before the start of phase 2 of testing for both the strengthened slabs to form the baseline for subsequent inspections. Details are given in [3].

4 Summary

The deck slabs with reinforcement representative of typical existing bridge decks were found to be susceptible to punching shear failure under field-representative wheel loads. Also it was evident that strengthening of individual components can cause other components to reach their limit state under higher load demands and prevent the strengthened component to reach ultimate capacity. Thus it can be concluded that to utilize the efficacy of the FRP strengthening, the design should consider the overall structural response at system level rather than treating it as a patch repair technique. The strengthening of components can also affect the load distribution as was indicated by the localization of damage and formation of through thickness cracks at intersections of the slab and the girder after strengthening of the slabs.

Acknowledgements

References

[1] Ghosh, K and Karbhari,, V.M."Evaluation of Strengthening Through Laboratory Testing of FRP Rehabilitated Bridge Decks After In-Service Loading," *Composite Structures*, 77[2], pp. 206-222, 2007.

[2] Ghosh, K.K., Lee, L., Karbhari, V.M.and Sikorsky, C. "Characterization of Effectiveness of Bridge Deck Rehabilitation," *Proceedings of the 4th International Conference on Advanced Composite Materials in Bridges and Structures,* Canada, 8 pp., 2004..

[3] Ghosh, K.K., "Assessment of FRP Composite Strengthened Reinforced Concrete Bridge Structures At the Component and Systems Level Through Progressive Damage and Non-Destructive Evaluation," Ph.D. dissertation, UCSD, 2006.

[4] AASHTO LRFD Bridge Design Specifications (2004), American Association of State Highway and Transportation Officials, Third Edition.

[5] Niu, H. and Wu, Z. (2001), "Prediction of Debonding Failure Load Due to Flexural Cracks in Concrete for FRP Strengthened Structures," Proceedings of FRPRCS-5, Cambridge, July, pp. 361-370.